

Effect of concentration quenching on the spectroscopic properties of $\text{Er}^{3+}/\text{Yb}^{3+}$ co-doped AlF_3 -based glasses

Junjie Zhang (张军杰), Shixun Dai (戴世勋), Shiqing Xu (徐时清),
Guonian Wang (汪国年), Liyan Zhang (张丽艳), and Lili Hu (胡丽丽)

Shanghai Institute of Optics and Fine Mechanics, Chinese Academy of Science, Shanghai 201800

Received March 18, 2004

A series of highly $\text{Er}^{3+}/\text{Yb}^{3+}$ co-doped fluoroaluminate glasses have been investigated in order to develop a microchip laser at $1.54 \mu\text{m}$ under 980 nm excitation. Measurements of absorption, emission and up-conversion spectra have been performed to examine the effect of $\text{Er}^{3+}/\text{Yb}^{3+}$ concentration quenching on spectroscopic properties. In the glasses with Er^{3+} concentrations below 10 mol%, concentration quenching is very low and the $\text{Er}^{3+}/\text{Yb}^{3+}$ co-doped fluoroaluminate glasses have stronger fluorescence of $1.54 \mu\text{m}$ due to the ${}^4I_{13/2} \rightarrow {}^4I_{15/2}$ transition than that of Er^{3+} singly-doped glasses. As Er^{3+} concentrations above 10 mol% in the $\text{Er}^{3+}/\text{Yb}^{3+}$ co-doped samples, concentration quenching of $1.54 \mu\text{m}$ does obviously occur as a result of the back energy transfer from Er^{3+} to Yb^{3+} . To obtain the highest emission efficiency at $1.54 \mu\text{m}$, the optimum doping-concentration ratio of $\text{Er}^{3+}/\text{Yb}^{3+}$ was found to be approximately 1:1 in mol fraction when the Er^{3+} concentration is less than 10 mol%.

OCIS codes: 160.5690, 160.4670, 300.6280, 160.2750, 160.3130.

Laser oscillators based on an erbium-doped laser system which can be operated in a microchip configuration^[1-3] have recently become the subject of great interest, especially for their potential use at $1.54 \mu\text{m}$ and for telemetry at an eye-safe wavelength. So far, microchip lasers at wavelengths of 1.06 ^[1,2] and $1.340 \mu\text{m}$ ^[3] have been mainly investigated in rare earth ions doped crystalline host materials. High power microchip laser operation in glass hosts requires that rare earth concentration should be at least one order of magnitude higher than those in crystalline hosts. This increase is required in order to obtain sufficient absorption of the pumping radiation in short active-length of material and to compensate for small gain^[1]. However, the occurrence of cluster and concentration quenching in high rare earth concentrations in most of glass systems are the major obstacle in this area^[1,4]. According to the above reasons, only several papers have been published since the first erbium doped glass-based microchip laser has been reported in 1993^[5]. To our knowledge, there are no reports that systematically analyzed the effect of concentration quenching on the spectroscopic properties of highly $\text{Er}^{3+}/\text{Yb}^{3+}$ co-doped fluoroaluminate glasses.

Fluoride glass is a good host for rare earth doping and to obtain high efficiency upconversion luminescence because of its lower phonon energy than oxide glasses^[6,7]. Fluoride glass also has more symmetric and smaller crystal fields than oxide glass systems^[8]. ZrF_4 -based (fluorozirconate) glasses and AlF_3 -based (fluoroaluminate) glasses are two main types of fluoride glasses. Most of the previous works are focusing on the ZrF_4 -based glasses with high Er^{3+} singly doped^[9-12]. In fact, Er^{3+} highly doped fluoroaluminate glass also has a strong $1.54\text{-}\mu\text{m}$ emission under 980-nm excitation^[13]. In addition, fluoroaluminate glass offers another important advantage over fluorozirconate glass for using as a laser host because of its higher glass transition temperature, and more chemically and mechanically durable than fluorozirconate^[14]. Furthermore, fluoroaluminate glass

systems have high ability to allow very high ytterbium-incorporation^[15].

The development of erbium glass laser systems has renewed the requirements for additional researches of improving laser glass properties and performance. It is well known that three-level laser system requires more population in the excited metastable level than that in the ground level. Because $1.54\text{-}\mu\text{m}$ Er^{3+} laser is a three-level laser system, so Yb^{3+} ion is always chosen as sensitizer for co-doping to achieve efficient laser operation. In the Yb^{3+} energy level scheme, there are only two manifolds, i.e., the ${}^2F_{7/2}$ ground state and the ${}^2F_{5/2}$ excited state. Yb^{3+} laser materials have a strong absorption peak, which is well coupled to a 980-nm InGaAs laser diode. It is commonly believed that, because of the simplest energy scheme of Yb^{3+} ion concentration quenching, excited state absorption, up-conversion and multi-phonon relaxation do not occur in this ion^[16]. In this work, Yb^{3+} is added to Er^{3+} doped fluoroaluminate glasses and the emission intensity depended upon Er^{3+} and Yb^{3+} concentration is investigated. The mechanism of energy-transfer between Er^{3+} and Yb^{3+} in high $\text{Er}^{3+}/\text{Yb}^{3+}$ co-doped fluoroaluminate glasses is also discussed. An optimum $\text{Er}^{3+}/\text{Yb}^{3+}$ concentration ratio is found experimentally.

A series of fluoroaluminate glass samples are prepared using reagent grade AlF_3 , MgF_2 , CaF_2 , SrF_2 , BaF_2 , YF_3 , ErF_3 and YbF_3 as the starting materials. The batch compositions of the glasses are listed in Table 1.

Accurately weighted 5-g batches are thoroughly mixed and moved into platinum crucibles. 10 wt % of ammonium bifluoride ($\text{NH}_4\text{F}\cdot\text{HF}$) is mixed with each batch. The batches are melted in the temperature range of 1000–1050 °C for 15 minutes under an Ar atmosphere. The melts are cast into preheated brass molds, and then the obtained glasses are annealed at their transition temperatures determined by differential thermal analysis (DTA). The glasses are cut into the size of $5 \times 5 \times 1 \text{ mm}^3$ for optical measurements.

Table 1. Composition of Glasses (mol%)

Glass	($x + y < 15.0$)	($x + y > 15.0$)
AlF ₃	35.0	35.0/(85+x+y)
MgF ₂	12.5	12.5/(85+x+y)
CaF ₂	12.5	12.5/(85+x+y)
SrF ₂	12.5	12.5/(85+x+y)
BaF ₂	12.5	12.5/(85+x+y)
YF ₃	15.0 - x - y	
ErF ₃	x	x
YbF ₃	y	y

$x = 0.5, 1.0, 3.0, 5.0, 7.0, 9.3, 11.9, 14.9, 18.2, 22.5, 26.0$;
 $y = 0.5, 1.0, 2.0, 3.0, 5.0, 7.0, 9.3, 10.0, 11.9, 14.9, 18.2, 22.5, 26.0$.

The DTA is performed with a Rigaku Thermo Plus TG-DTA TG8110 apparatus under Ar atmosphere at a heating rate of 10 K·min⁻¹. Absorption spectra are measured with a SHIMADZU UV-2200 spectrophotometer. The 1.54- μ m emission spectra are obtained by excitation with a 980 nm InGaAs laser diode. Up-conversion luminescence spectra are measured with a HITACHI F-3010 fluorescence spectrophotometer under the 980 nm excitation. The spectra are recorded in similar experimental conditions, and the relative errors in these spectra measurements are estimated to be $< \pm 5\%$. All measurements are carried out at room temperature.

Figure 1 illustrates the observed absorption cross-section of the glasses with the compositions of 35.0AlF₃·12.5MgF₂·12.5CaF₂·12.5SrF₂·12.5BaF₂·10.0YF₃·5.0ErF₃ and 35.0AlF₃·12.5MgF₂·12.5CaF₂·12.5SrF₂·12.5BaF₂·5.0YF₃·5.0ErF₃·5.0YbF₃ in the range of 3500–30000 cm⁻¹. The observed spectra consist of thirteen absorption bands from the ⁴I_{15/2} ground state to the ⁴I_{13/2}, ⁴I_{11/2}, ⁴I_{9/2}, ⁴F_{9/2}, ⁴S_{3/2}, ²H_{11/2}, ⁴F_{7/2}, ⁴F_{5/2}, ⁴F_{3/2}, ²H_{9/2}, ⁴G_{11/2}, ⁴G_{9/2}, and ²G_{7/2} excited states, respectively. The absorption cross section around 10250 cm⁻¹ (980 nm) due to the Yb³⁺: ²F_{5/2} ← ²F_{7/2} transition is stronger than that due to the Er³⁺: ⁴I_{11/2} ← ⁴I_{15/2} transition. The absorption cross section around 980 nm in the Er³⁺/Yb³⁺ co-doped glass is 0.75×10^{-20} cm², which is larger than that 0.14×10^{-20} cm² in the Er³⁺ singly-doped glass. This indicates that

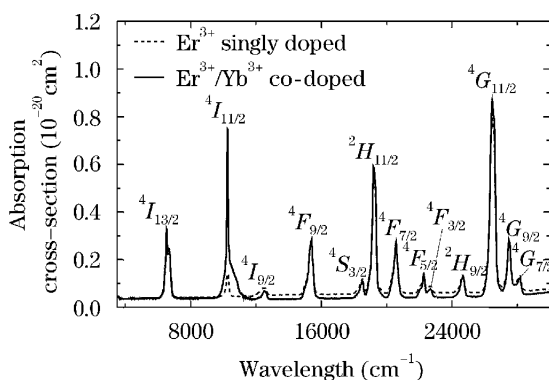


Fig. 1. Calculated absorption cross-section of Er³⁺ singly doped and Er³⁺/Yb³⁺ co-doped AlF₃-based glasses. The concentration of Er³⁺ and Yb³⁺ is 5 mol%, respectively.

the Er³⁺/Yb³⁺ co-doped fluoroaluminate glasses have higher absorption efficiencies than the Er³⁺ singly doped glasses under 980-nm excitation and the Yb³⁺ ion is particularly suitable in order to efficiently transfer its excitation energy to the Er³⁺ ion.

A high power and high efficiency microchip laser requires that the Er³⁺ concentration should be sufficiently high to ensure a net gain with such a thin (several hundred micrometer) active material. Because of the serious clustering and concentration quenching, it is difficult to obtain a high gain at 1.54 μ m in a microchip laser based on glasses with a doping of high concentrations of rare earth ions. Since Yb³⁺ has only one excited state of ²F_{5/2}, which locates at about 980 nm above the ground state of ²F_{7/2}, no concentration quenching occurs among the Yb³⁺ ions. An idea of the use of rare earth co-doping is to take advantage of the fact that Yb³⁺ acts as a sensitizer for Er³⁺. The mechanism has been known from a long time ago^[17]. Figure 2 shows the fluorescence emission spectra of the Er³⁺ singly doped and Er³⁺/Yb³⁺ co-doped fluoroaluminate glasses in the range of 1400–1700 nm under 980-nm excitation. As seen from Fig. 2, the strong Er³⁺: ⁴I_{13/2} → ⁴I_{15/2} fluorescence is observed around 1.54 μ m in both Er³⁺ singly doped and Er³⁺/Yb³⁺ co-doped glasses, and the 1.54- μ m emission intensity increases with increasing Yb³⁺-addition when the Yb³⁺/Er³⁺ concentration ratio does not exceed 1:1. Therefore, it may be expected to obtain higher gain in the addition of Yb³⁺ ion to the Er³⁺ singly doped fluoroaluminate glasses in this work.

In glasses with low Er³⁺ concentration doping (below 10 mol%), the Er³⁺: 1.54 μ m fluorescence intensity depends upon the Er³⁺ concentration in the Er³⁺ singly doped and Er³⁺/Yb³⁺ co-doped glasses under 980-nm excitation are shown in Fig. 3. In the Er³⁺/Yb³⁺ co-doped glasses the concentration ratio of Er³⁺/Yb³⁺ is 1:1. It can be seen that concentration quenching begins to occur slightly when the Er³⁺ concentration is up to about 5 mol%. However, in both of the Er³⁺ singly doped and Er³⁺/Yb³⁺ co-doped glasses, no concentration quenching is evidently observed even the Er³⁺ concentration reaches about 10 mol%. Wetenkam *et al.* have reported that concentration quenching easily occurs from the ⁴I_{11/2}

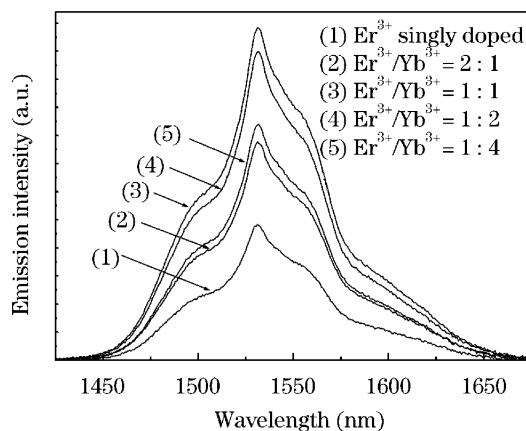


Fig. 2. Fluorescence spectra around 1.54 μ m of Er³⁺ singly doped and Er³⁺/Yb³⁺ co-doped glasses under 980-nm excitation. The Er³⁺ concentration is 10 mol% and the Er³⁺/Yb³⁺ concentration ratio is 0, 2:1, 1:1, 1:2, and 1:4 respectively.

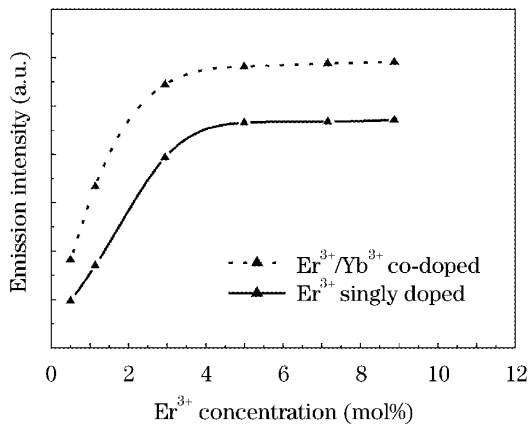


Fig. 3. Dependence of fluorescence intensity at $1.54 \mu\text{m}$ upon Er^{3+} concentration in Er^{3+} single doped and $\text{Er}^{3+}/\text{Yb}^{3+}$ co-doped AlF_3 -based glasses under 980-nm excitation. The $\text{Er}^{3+}/\text{Yb}^{3+}$ concentration ratio is 1:1.

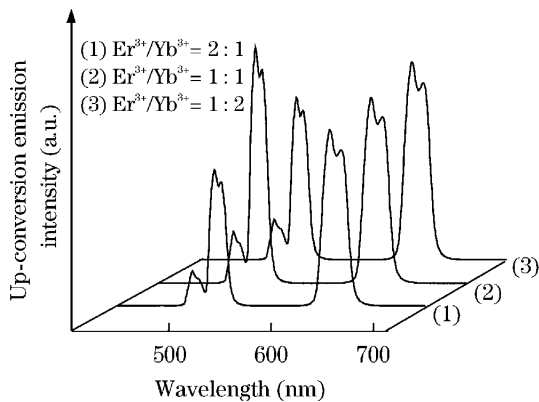


Fig. 4. Dependence of up-conversion luminescence intensity upon $\text{Er}^{3+}/\text{Yb}^{3+}$ concentration ratio in $\text{Er}^{3+}/\text{Yb}^{3+}$ co-doped AlF_3 -based glasses. The Er^{3+} concentration is 10 mol%.

and $^4I_{13/2}$ levels when the Er^{3+} concentration exceeds 4 mol% in ZBLAN glasses^[18]. The present highly $\text{Er}^{3+}/\text{Yb}^{3+}$ co-doped fluoroaluminate glasses give intense fluorescence efficiency at $1.54 \mu\text{m}$ and low concentration quenching. This fact may be considered to be a hopeful host for a $1.54\text{-}\mu\text{m}$ microchip laser and other optical laser applications.

On the other hand, up-conversion phenomenon takes place in a low phonon energy matrix, and brings some loss mechanisms for the infrared emission. The up-conversion emission spectra of $\text{Er}^{3+}/\text{Yb}^{3+}$ co-doped glasses under 980-nm excitation are shown in Fig. 4. In the glasses the concentration of Er^{3+} is fixed to 10 mol% and the concentration ratio of $\text{Er}^{3+}/\text{Yb}^{3+}$ is changed from 2:1 to 1:2. According to the Er^{3+} energy levels, the green (around 550 nm) and red (around 660 nm) emission bands correspond to the transitions from the ($^4H_{11/2}$, $^4S_{3/2}$) and $^4F_{9/2}$ states to the $^4I_{15/2}$ ground state, respectively. The red emission intensity increases while the green emission intensity decreases with an increase in the Yb^{3+} concentration in $\text{Er}^{3+}/\text{Yb}^{3+}$ co-doped glasses.

An energy-transfer mechanism proposed for the $\text{Er}^{3+}/\text{Yb}^{3+}$ co-doped glasses is schematically depicted in Fig. 5. The Yb^{3+} ion has only one excited manifold ($^2F_{5/2}$ level) located at approximately 10000 cm^{-1} .

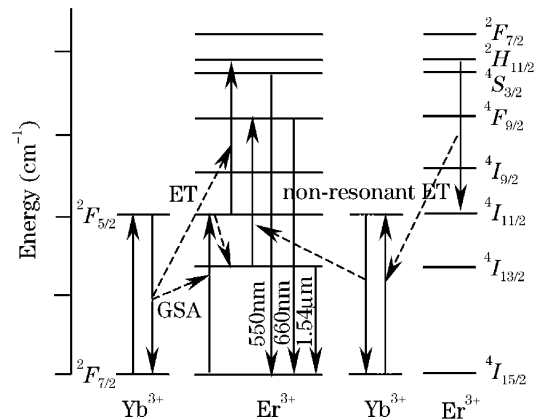


Fig. 5. Schematic diagram of energy transfer between Er^{3+} and Yb^{3+} in $\text{Er}^{3+}/\text{Yb}^{3+}$ co-doped AlF_3 -based glasses. The upward and downward arrows indicate photon absorption and fluorescence emission, respectively.

When excitation is performed at the $^2F_{7/2}$ level of Yb^{3+} with a diode laser operating at 980 nm, the Yb^{3+} emission band due to the $^2F_{5/2} \rightarrow ^2F_{7/2}$ transition just overlaps the Er^{3+} absorption band due to the $^4I_{11/2} \rightarrow ^4I_{15/2}$ transition, indicating the energy transfer from Yb^{3+} to Er^{3+} in the glasses.

In the first step of energy-transfer, the excited Yb^{3+} ions transfer their energies to Er^{3+} ions, the $4f$ electrons that are on the $^4I_{15/2}$ ground state are excited to the $^4I_{11/2}$ level, and the $1.54\text{-}\mu\text{m}$ emission is observed due to the $^4I_{13/2} \rightarrow ^4I_{15/2}$ transition after a multi-phonon relaxation process. The $4f$ -electrons on the $^4I_{11/2}$ level reach to the $^2H_{11/2}$ level by absorbing another photon due to the $^2F_{5/2} \rightarrow ^2F_{7/2}$ transition. The green and red emissions, which are due to the ($^2H_{11/2}$, $^4S_{3/2}$) $\rightarrow ^4I_{15/2}$ and $^4F_{9/2} \rightarrow ^4I_{15/2}$ transitions, respectively, are observed. In the high $\text{Er}^{3+}/\text{Yb}^{3+}$ dopant values, non-resonant energy-transfer occurs from Er^{3+} to Yb^{3+} when high population of Er^{3+} ions on the $^2H_{11/2}$ state occurs at the same time. In this energy-transfer process, Yb^{3+} ions that absorbed the energy from Er^{3+} transfer the energies to another neighboring Er^{3+} ions that on the $^4I_{13/2}$ level, and then the Er^{3+} ions are excited to the $^4F_{9/2}$ level. Since the population on the $^4I_{13/2}$ state is reduced, the red emission intensity increases, while the $1.54\text{-}\mu\text{m}$ emission intensity decreases. Therefore, an optimum concentration ratio of $\text{Er}^{3+}/\text{Yb}^{3+}$ is desired for highly $\text{Yb}^{3+}/\text{Er}^{3+}$ doped fluoroaluminate glasses. Based on the present experimental result, the best $\text{Er}^{3+}/\text{Yb}^{3+}$ doping ratio is 1:1 in mol% when the Er^{3+} concentrations is below 10 mol%. Since the concentration quenching due to the back energy-transfer from Er^{3+} to Yb^{3+} rapidly occurs when the Er^{3+} concentration is above 10 mol%, the Yb^{3+} concentration should be lowered to obtain higher $1.54\text{-}\mu\text{m}$ emission efficiency of Er^{3+} .

In addition, an increase of the Yb^{3+} concentration in the low dopant value will result in an increased non-radiative energy-transfer from Yb^{3+} to Er^{3+} , improving the Er^{3+} : $1.54\text{-}\mu\text{m}$ emission efficiency. In the high dopant value, however, excessive Yb^{3+} concentration will cause an increase in the back energy-transfer from

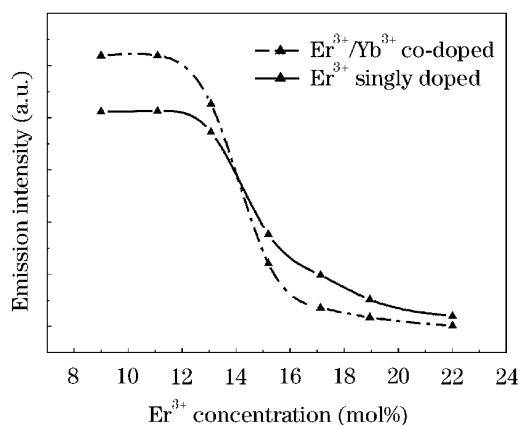


Fig. 6. Dependence of 1.54- μm fluorescence intensity upon Er^{3+} concentration in $\text{Er}^{3+}/\text{Yb}^{3+}$ co-doped AlF_3 -based glasses with high dopant contents. The $\text{Er}^{3+}/\text{Yb}^{3+}$ concentration ratio is 1:1.

Er^{3+} to Yb^{3+} . It can be found that the fluorescence intensity of $\text{Er}^{3+}/\text{Yb}^{3+}$ co-doped glasses decreases very faster than that of Er^{3+} singly doped glasses when the Er^{3+} concentration exceeds 10 mol%, as shown in Fig. 6. In highly Er^{3+} singly doped glasses, the decrease is due to cross relaxation between two neighboring Er^{3+} ions. In highly $\text{Er}^{3+}/\text{Yb}^{3+}$ co-doped glasses, the decrease in Er^{3+} emissions including 1.54- μm emission, the green and red up-conversion luminescence indicates that excitation energies are transferred from Er^{3+} to Yb^{3+} . The rate of energy transfer by a dipole-dipole interaction is obtained by the Dexter equation^[19] described as follows

$$P_{\text{SA}} = \frac{3\eta c^2 Q_A Q_S}{4\pi^3 n^2 R^6} \int \frac{f_S(E) f_A(E)}{E^2} dE, \quad (1)$$

where n is the refractive index, R is the average distance between the sensitizer and activator, Q_A and Q_S are the integrated absorption and emission cross sections of activator and sensitizer, respectively, and f_A and f_S are the normalized line shape functions of the absorption and emission spectra of the same ions. In high Er^{3+} and Yb^{3+} dopant contents, as can be seen from Fig. 6, the back energy-transfer process becomes more significant since the distance R between Er^{3+} and Yb^{3+} becomes closer. This leads to a situation that the 1.54- μm emission intensity becomes much weaker in highly $\text{Er}^{3+}/\text{Yb}^{3+}$ co-doped glasses than in Er^{3+} singly doped glasses.

In conclusion, the effects of $\text{Er}^{3+}/\text{Yb}^{3+}$ concentration quenching on the spectroscopic properties are investigated in the highly $\text{Er}^{3+}/\text{Yb}^{3+}$ co-doped fluoroaluminate glasses by the 980-nm excitation. Strong 1.54- μm emission is observed in both of the Er^{3+} singly doped and $\text{Er}^{3+}/\text{Yb}^{3+}$ co-doped glasses, and no concentration quenching is obviously observed even the Er^{3+} concentration reaches about 10 mol%.

In the glasses with Er^{3+} concentrations below 10 mol%, concentration quenching is low and the $\text{Er}^{3+}/\text{Yb}^{3+}$ co-doped fluoroaluminate glasses have high quantum efficiency and strong fluorescence at 1.54 μm which corresponds to the Er^{3+} : ${}^4I_{13/2} \rightarrow {}^4I_{15/2}$ transition than

that of Er^{3+} singly-doped glasses.

In the glasses with Er^{3+} concentration above 10 mol%, concentration quenching of 1.54 μm occurs more obviously than that of the Er^{3+} singly-doped samples as a result of the back energy-transfer from Er^{3+} to Yb^{3+} and higher probabilities of the cross relaxation between Er^{3+} ions. Consequently the fluorescence intensity at 1.54 μm decreases, while the red up-conversion emission intensity increases and the green upconversion emission intensity decreases. To obtain the highest emission efficiency at 1.54 μm , the best doping-concentration ratio $\text{Er}^{3+}/\text{Yb}^{3+}$ is found to be approximately 1:1 in mol fraction when the Er^{3+} concentration is less than 10 mol%. The glasses presented here are considered to be an excellent candidate for the use as compact optically pumped eye-safe microchip lasers.

This work was supported by the Rising-Star Project (No. 04QMX1448) of Shanghai Municipal Science and Technology Commission and the National Natural Science Foundation of China (No. 60207006). J. Zhang's e-mail address is zjj@laserglass.com.cn.

References

1. D. R. MacFarlane, J. Javorniczky, P. J. Newman, V. Bogdanov, D. J. Booth, and W. E. K. Gibbs, *J. Non-Cryst. Solids* **213&214**, 158 (1997).
2. M. Qiu, J. B. David, W. B. Gregory, and C. B. Glenn, *Appl. Opt.* **32**, 2085 (1993).
3. T. Taira, A. Mukai, Y. Nozawa, and T. Kobayashi, *Opt. Lett.* **16**, 1955 (1991).
4. F. Lin, H. Hu, G. Yi, and J. Feng, in *Proceeding of 8th International Symposium on Non-Oxide Glass* 364 (1992).
5. P. Laporta, S. Taccheo, S. Longhi, and O. Sevito, *Opt. Lett.* **18**, 1232 (1993).
6. F. Gan, *J. Non-Cryst. Solids* **184**, 9 (1995).
7. D. C. Hanna and A. C. Troppier, in *Optical Fibers Lasers and Amplifiers* P. W. France and Blackie (eds.) (CRC Press, London, 1991) p. 164.
8. W. J. Miniscalco, *J. Lightwave Technol.* **9**, 234 (1991).
9. V. K. Bogdanow, W. E. K. Gibbs, D. J. Booth, J. S. Javorniczky, P. J. Newman, and D. R. Macfarlane, *Opt. Commun.* **132**, 73 (1996).
10. X. Zuo and T. Izumitani, *J. Non-Cryst. Solids* **162**, 68 (1993).
11. M. Tsuda, K. Goga, H. Inoue, S. Inoue, and A. Makishima, *J. Appl. Phys.* **86**, 6143 (1999).
12. K. Soga, M. Tsuda, and S. Sakuragi, *J. Non-Cryst. Solids* **222**, 272 (1997).
13. L. Zhang, H. Hu, and F. Lin, *Mater. Lett.* **47**, 189 (2001).
14. G. H. Frischat, B. Hueber, and B. Rahmdohr, *J. Non-Cryst. Solids* **284**, 105 (2001).
15. R. S. Quimby, *Electron. Lett.* **23**, 32 (1987).
16. D. S. Snmida and T. Y. Fan, *Opt. Lett.* **19**, 1343 (1994).
17. F. E. Auzel, *Proc. IEEE* **61**, 758 (1973).
18. L. Wetenkam, G. F. West, and H. Tobben, *J. Non-Cryst. Solids* **140**, 30 (1992).
19. D. L. Dexter, *J. Chem. Phys.* **21**, 836 (1953).